Multiobjective Genetic Optimization of Terrain-Independent RFMs for VHSR Satellite Images

Amin Alizadeh Naeini, Sayyed Hamed Alizadeh Moghaddam, Sayyed Mohammad Javad Mirzadeh, Saeid Homayouni, *Senior Member, IEEE*, and Sayyed Bagher Fatemi

***Abstract*— Rational polynomial coefficients (RPCs) biases and over-fitting phenomenon are two major issues in terrain-independent rational function models. These problems degrade the accuracy of extracted spatial information from very high spatial resolution (VHSR) satellite images. This study particularly focused on overcoming the over-fitting problem through an optimal term selection approach. To this end, multiobjective genetic algorithm was used in order to optimize three effective objective functions: the RMSE of ground control points (GCPs), the number, and the distribution of both RPCs and GCPs. Finally, the technique for order of preference by similarity to ideal solution, as an efficient multicriteria decision-making method, was applied to select the best solution, i.e., the optimum terms of RPCs, through the ranking of solutions in the optimum set. The performance of the proposed method was evaluated by using three VHSR images acquired by GeoEye-1, Worldview-3, and Pleiades satellite sensors. Experimental results show that subpixel accuracy can be nearly achieved in all data sets, when over-fitting problem is addressed. The optimal selected terms leaded to a significant improvement compared to the original RPCs. Indeed, our method, which is independent of GCPs distribution, not only requires a small number of GCPs, but also leads to a 30% to 75% improvement when compared to the original RPCs. This improvement in VHSR images, usually makes no more need to remove the RPCs biases.**

***Index Terms*— Decision analysis, multiobjective genetic algorithm (MOGA), over-fitting, rational function models (RFMs).**

I. Introduction

THANKS to their high geometric accuracy, very high spatial resolution (VHSR) satellite images are beneficial data for many applications such as image matching, georeferencing, orthorectification, and digital elevation model (DEM) generation [1]. Specially, the role of these data becomes more significant where aerial photogrammetry is not feasible due to the political or geographical restrictions [2]. For all precise mapping purposes, knowing the geometric relationship between 2-D image space and 3-D ground space is essential.

Among different proposed models addressing this geometric relationship, rational function model (RFM) is one of the most well-defined, robust, and frequently used models [3]. This model is indeed a ratio between two third-order polynomials with 80 rational polynomial coefficients (RPCs), containing the essential information about the sensor and the satellite platform, including the position and the attitude information [1], [3].

From the perspective of the way through which the RPCs are estimated, RFMs can be classified into the two main categories: terrain-dependent and terrain-independent models [1], [3], [4]. In terrain-dependent models, RPCs should be normally estimated using a number of well-distributed ground control points (GCPs), while in the second models, they are estimated based on the auxiliary information provided by inertial navigation system, on-board GPS receivers, and stellar cameras.

Terrain-dependent models, in addition to the sensitivity to the number and the distribution of GCPs, severely suffer from over-fitting phenomenon. Terrain-independent models, on the other hand, suffer from not only over-fitting phenomenon, but also the RPCs biases [5], [6]. In these two models, over-fitting comes from the vast number of RFM's parameters and their strong correlation [7], [8]. To address the over-fitting issue which leads to accuracy degradation in the case of terrain-independent model, data providers are strongly recommended to apply the optimization methods to RPCs generation, in order to select the optimum coefficients for each image.

Several solutions have been proposed in the literature for the over-fitting problem in the case of terrain-dependent models, such as regularization methods [9], [10], like ridge estimation [3], [11]–[13], Levenberg–Marquardt method [3], [14], and parameter reduction or optimum term selection techniques through the optimization-based methods [15]–[17].

Tao and Hu [3] have investigated both terrain-independent and terrain-dependent models. Their investigation demonstrates that the terrain-dependent model can achieve a good approximation accuracy, are adequate and evenly distributed [3], which is not practically easy. Zhang *et al.* [1] have suggested a method to automatically optimize RFM parame-

Manuscript received April 2, 2017; revised May 16, 2017; accepted June 1, 2017. Date of publication July 6, 2017; date of current version July 20, 2017. *(Corresponding author: Amin Alizadeh Naeini.)*

A. Alizadeh Naeini and S. B. Fatemi are with the Department of Geomatics Engineering, Faculty of Civil Engineering and Transportation, University of Isfahan, Isfahan 8174673441, Iran (e-mail: a.alizadeh@eng.ui.ac.ir; sb.fatemi@eng.ui.ac.ir).

S. H. Alizadeh Moghaddam and S. M. J. Mirzadeh are with the Faculty of Geodesy and Geomatics Engineering, K. N. TOOSI University of Technology, Tehran 1996715433, Iran (e-mail: h.alizadeh@email.kntu.ac.ir; smjmirzadeh@mail.kntu.ac.ir).

S. Homayouni is with the Department of Geography, Environment, and Geomatics, University of Ottawa, ON K1N 6N5, Canada (e-mail: saeid.homayouni@uOttawa.ca).

Color versions of one or more of the figures in this letter are available online at http://ieeexplore.ieee.org.

Digital Object Identifier 10.1109/LGRS.2017.2712810

1545-598X © 2017 IEEE. Personal use is permitted, but republication/redistribution requires IEEE permission.
See http://www.ieee.org/publications_standards/publications/rights/index.html for more information.

ters by a stepwise selection of the necessary parameters, based on the scatter matrix and the elimination transformation strategies. Long *et al.* [7] have presented the nested regression-based optimal selection for selecting optimal RPCs automatically, and obtaining the stable solutions for the terrain-dependent RFM. A serious drawback with this method is that it is a local-search method, which may not result in an optimum solution [7]. In addition, it needs a relatively high number of GCPs.

Yuan and Cao [18] have proposed an optimized method to select RPCs. This method is, indeed, a variable selecting method based on the evaluation criteria of multicollinearity [18]. To estimate the RPCs, Long *et al.* [8] have applied L1-norm-regularizad least squares which provides stable results in both terrain-dependent and terrain-independent models. The main deficiency of this method is regularization parameter, which is empirically selected, and is rarely optimal [8].

In addition, several works have been done based on L1-norm regularization, including least absolute shrinkage and selection operator [19], basis pursuit denoising [20], least angle regression [21], and the elastic net [22]. These robust and efficient methods normally result in a unique solution of RPCs, especially with insufficient number of observations. Several research works, based on the artificial intelligence algorithms, have also been purposed for RFM optimal term selection [15]. Valadan Zoej *et al.* [17] and Yavari *et al.* [16] have used genetic algorithm (GA) and the modified particle swarm optimization, respectively.

All of these cited approaches do not use the vendor-provided RPCs, which nowadays are an inseparable part of every satellite imagery product. Therefore, the coefficients of RFMs in each image must be estimated, which is computationally expensive [16]–[18]. Furthermore, these methods do not directly consider the number and the distribution of GCPs as well as the number of RPCs, as the main influencing factors on the final accuracy.

To overcome the over-fitting problem in terrain-independent models, in this letter, an innovative tri-objective GA optimization was proposed in which: 1) the number of GCPs; 2) the number of RPCs; and 3) GCP RMSE are simultaneously minimized. The first objective was to address the problem of number and distribution of GCPs. By doing this, we tried to find the optimum GCPs as well as to address the dependence of the results to the number and the distribution of the GCPs. Second objective was the number and distribution of RPCs. The RPCs position and their number, as significant factors on over-fitting phenomenon, were regarded. Third and last objective of the proposed method, was RMSE minimization, estimated from GCPs. However, since the output of multiobjective GA (MOGA) is a set of optimal solutions, a dominant multicriteria decision making, namely, the technique for order of preference by similarity to ideal solution (TOPSIS), was used for ranking pareto front solution.

II. Proposed Method

A novel two-stage method, which is actually the integration of MOGA [3] and TOPSIS [23], [24], is proposed in the interest of RFM optimal term selection. In the RFM, the image pixel coordinates (l, s) are expressed as the ratios of two third-order polynomials of ground coordinates (X, Y, Z). For the ground-to-image transformation, the RFM can be described as follows:

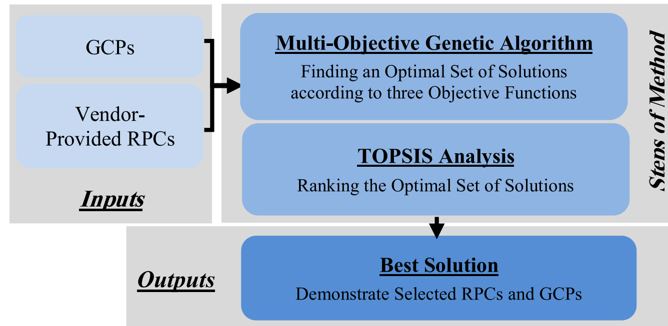

Fig. 1. Flow diagram of the proposed method.

TABLE I
GA Parameters Used in the Algorithm Implementation

Parameters	Value or Option
Pareto Fraction	0.3
Distance Measurement Function	genotype distance-crowding
Creation of Population	uniform distribution function
Selection of Pareto	tournament approach
Population Size	100
Crossover Fraction	0.8
Migration Interval	5
Migration Fraction	0.6

$$\begin{aligned} l_n &= p_1(X_n, Y_n, Z_n)/p_2(X_n, Y_n, Z_n) \\ s_n &= p_3(X_n, Y_n, Z_n)/p_4(X_n, Y_n, Z_n) \end{aligned} \tag{1}$$

where (l_n, s_n) are the normalized line and sample of pixels in image space, (X_n, Y_n, Z_n) are normalized coordinate values of object points, and $p_1, p_3, p_2,$ and p_4 are 20-term cubic polynomials.

Fig. 1 shows the flow diagram of the proposed method. To use MOGA: 1) the parameters of MOGA (Table I); 2) chromosome representation (P_t); and 3) the objective functions have to be defined, which are as follows:

$$f_1 = RMSE \quad . f_2 = nGCPs \quad . f_3 = nRPCs$$

$$P_t = \begin{array}{|c|c|c|c|c|c|c|c|c|c|} \hline RP_1 & .... & RP_k & .... & RP_{NRPCs} & GC_1 & .... & GC_k & .... & GC_{NGCPs} \\ \hline \end{array}$$

In which, RP_k and GC_k are set to 1 or 0 (binary format). The size of P_t is equal to the sum of the RPCs and the GCPs numbers (nRPCs + nGCPs), f_1 is the RMSE of GCPs, f_2 and f_3 are the numbers of GCPs and RPCs, respectively.

Finally, the TOPSIS was used to find the best solution among the solutions found by MOGA. To use TOPSIS, a decision matrix should be first formed for the considered problem. The matrix's rows and columns indicate the alternatives and

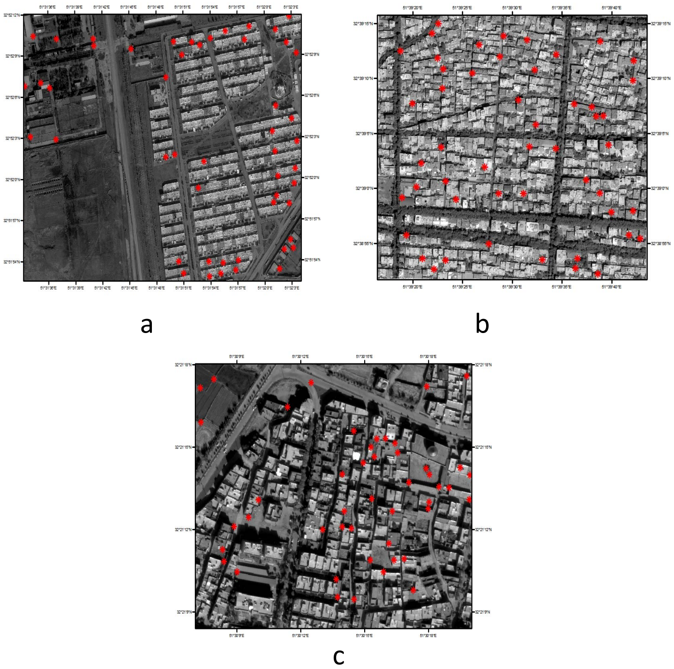

Fig. 2. Three VHSR data sets. (a) GeoEye-1 subscene of Shahinshahr, Isfahan. (b) Pleiades subscene of Isfahan's downtown Isfahan. (c) WorldView-3 subscene of Mobarakeh, Isfahan, Iran.

the criteria, respectively. The alternatives are a set of optimal solutions found by MOGA, while the criteria are as follows.

1) *RMSE Index:* This is the line, sample, and total RMSE (i.e., the average of RMSEs along the line and sample direction [25]) of GCPs, which were used in the process of MOGA optimization.
2) *Total standard deviation (STD) Index:* This represents the line, sample, and STD of the selected GCPs in the optimization.
3) *Number of GCPs:* This is the number of GCPs selected by MOGA.
4) *Number of RPCs:* This index is the number of RPCs, resulted as one of the outputs of RFM optimization by MOGA.

III. Experimental Results

In this part, used data sets are presented at first. Parameter tuning of the proposed method is explained afterwards. Finally, obtained results are discussed.

A. VHSR Data Sets

The remote sensing data sets used in this letter includes three VHSR panchromatic images from GeoEye-1, WorldView-3, and Pleiades satellites. The spatial resolution of all images is about 50 cm. All images were extracted from the original scene data and the RPCs were recalculated for the subscenes. These images are from different urban areas in Isfahan province, Iran. The satellite images as well as the GCPs as red points are presented in Fig. 2.

For each case study, a 1:2000 digital reference map was used for 3-D coordinate collection of GCPs. All these maps have been produced through the photogrammetric stereo plotting from the aerial photographs.

TABLE II

Line, Sample, and Total RMSE and STD Values for the Three Data Sets in the Case of Original RPCs

Satellite Data	RMSE (pixel)			STD (pixel)		
	Line	**Sample**	**Total**	**Line**	**Sample**	**Total**
GeoEye-1	0.48	2.20	1.34	0.39	0.80	0.60
Pleiades	3.03	1.42	2.23	0.71	0.49	0.60
WorldView-3	4.62	2.13	3.38	0.43	0.60	0.51

B. Parameter Setting

Prior to running any population-based optimization methods like MOGA, several parameters must be set. The first parameter is either the number of iterations or stopping criterion. In this research, the value of average change in the spread of pareto front was used. As a result, the algorithm stops, if this value over sixty generations is less than 10^{-6} for function tolerance [26]. Another important parameter is the elitism, controlled by both pareto fraction and the distance measurement function options. Other parameters of the MOGA are presented in Table I. It should be noted that these suggested parameter values and options are frequently used in [27]–[30].

Ranking by TOPSIS completely depends on the weighting method. Therefore, here, we applied one of the simplest, widely used, weighting strategies, which is the inverse of the number of selected indices.

C. Results and Discussion

Since the RPCs provided with VHSR images are not accurate due to RPCs biases and over-fitting phenomenon, in this part, the accuracy of the original RPCs was primarily estimated for each data set. RPCs were then refined using one GCP. Last, the results of the proposed method, presented to address over-fitting phenomenon, are discussed. To perform a more accurate evaluation, we applied two well-known quality assessment parameters (QAPs), i.e., RMSE and STD of check points. RMSE and STD were, respectively, selected to assess the overall accuracy and the reliability of methods in question.

1) Original RPCs: In this stage, all of the coefficients, provided originally with the data, were used in order to solve RFM. Two QAPs, computed from 25 check points for each data set, are presented in Table II. The results show that by all RPCs, RFM could not lead to the subpixel accuracy for any of these three data sets. This is mainly due to the RPCs biases and over-fitting problem.

2) RPCs Refinement: To obtain the refined coefficients, RPCs biases removal was performed by only one GCP. Several researches have shown that one GCP is sufficient for RPCs refinement of VHSR images [6], [31], [32]. For this purpose, 50-fold cross validation was applied. Because the number of GCPs is equal to 50. In each cross validation, as discussed, one point was regarded as training set for RPCs refinement

TABLE III
LINE, SAMPLE, AND TOTAL RMSE AND STD VALUES FOR THE THREE DATA SETS IN THE CASE OF RPCs REFINEMENT

Satellite Data	RMSE (pixel)			STD(pixel)		
	Line	Sample	Total	Line	Sample	Total
GeoEye-1	0.59	1.12	0.85	0.59	1.12	0.85
Pleiades	0.96	0.64	0.80	0.96	0.64	0.80
WorldView-3	0.66	0.93	0.80	0.66	0.93	0.80

TABLE IV
TOPSIS BEST SOLUTIONS FOR RMSE AND STD OF GCPs AND ICPs

Satellite Data		RMSE Of GCPs	STD Of GCPs	RMSE Of ICPs	STD Of ICPs
GeoEye-1	***Line***	0.12	0.07	0.45	0.39
	Sample	0.01	0.01	1.19	0.87
	Total	0.06	0.04	0.82	0.63
Pleiades	***Line***	1.69	0.23	2.62	0.70
	Sample	0.08	0.04	0.68	0.58
	Total	0.88	0.13	1.65	0.64
WorldView-3	***Line***	0.07	0.09	0.95	0.42
	Sample	0.02	0.00	0.88	0.64
	Total	0.04	0.05	0.91	0.53

(zero-order). Cross validation was then applied to show how much RPCs refinement depends on the GCPs distribution.

Table III represents the RMSE and STD values for all data sets. As it can be seen, although the subpixel accuracy has been obtained by RPCs biases removal for all the three data sets, the STD values are not satisfying. According to the RMSE results of Table III, the refined RPCs with subpixel accuracy outperformed the original RPCs (Table II). The STD values, however, increased by 35%. Therefore, RPCs biases removal with one point cannot lead to reliable results. In addition, the STD values are quite large, although their RMSE are less than one pixel (see Table III). In other words, for all the three data sets, the refinement completely depends on the GCPs' distribution.

3) Optimum RPCs Selection: Optimal terms selection of the originally provided RPCs by the proposed method is the third stage of the implementation. A set of optimal solutions (i.e., pareto front curves) for the three data sets are the results of MOGA optimization method.

To rank and select the best MOGA's solution, we used TOPSIS analysis. To use this analysis, we need to construct a decision matrix. The rows of matrix are solutions found by MOGA, and the columns include indices, which are explained at the end of the Section III. The characteristics of the best solution, selected by TOPSIS (i.e., RMSE of GCPs and independent check points (ICPs), number of RPCs and GCPs, and STD of GCPs and ICPs) are presented in Tables IV and V.

Compared to the RPCs biases removal stage, the optimal RPCs selection by MOGA leads better results in terms of RMSE and STD values for GeoEye-1 and Worldview-3 data sets. This approach improved the STD values by 30%, 25%, and 40% for GeoEye-1, Pleiades, and Worldview-3 data sets, respectively. The results presented in Table V show that the subpixel accuracy can be achieved by solely selecting 10 and 13 of the originally provided coefficients for GeoEye-1 and Worldview-3 data sets, respectively. The error in the first stage (i.e., original RPCs) is due to both over-fitting and RPCs biases. In GeoEye-1 and Worldview-3 data sets, subpixel accuracy is achieved when over-fitting problem is addressed by optimum term selection. Consequently, there is no need to concern about RPCs biases. However, in Pleiades data, although the proposed method leads to a significant improvement (about one pixel), RPCs biases should be removed to reach to subpixel accuracy.

TABLE V
TOPSIS BEST SOLUTIONS FOR THE NUMBER OF GCPs AND RPCs

Satellite Data	Number of RPCs				Number of GCPs
	Line_NUM	***Line_DEN***	***Sample_NUM***	***Sample_DEN***	
GeoEye-1	4	2	3	1	2
Pleiades	5	2	6	2	2
WorldView-3	6	2	4	1	2

IV. CONCLUSION

Nowadays, modern and high-resolution remote sensing systems provide RFMs as an essential component of the satellite imagery. This information is widely used for georeferencing, DEM generation, and ortho-map production. However, RFMs have two major problems, RPCs biases and over-fitting phenomenon, which degrade the accuracy of geospatial information extracted from these imageries. Accordingly, in order to obtain reliable and accurate remote sensing products, these issues must be addressed in a way that lead to pixel or subpixel accuracy level.

Among these two issues, the over-fitting problem was addressed in this letter. To tackle this problem, we proposed a novel two-stage method which is actually the integration of an optimization algorithm and decision analysis. The proposed method indeed could find the best combination of vendor-provided RPCs with minimum mutual correlations as well as the optimum distribution of GCPs. The experimental tests revealed that about one-pixel accuracy with high reliability can be achieved with only 10 to 15 of RPCs and only two GCPs. By this improvement, the RPCs biases can be almost ignored in VHSR satellite images. In addition, the results showed that the optimal RPCs can lead to 30% to 75% improvement compared to the original RPCs accuracy. The proposed method showed also to be more reliable, compared to RPCs refinement, for all three VHSR satellite images. However, its accuracy was nearly the same as the refined RPCs, expect the case of Pleiades VHSR satellite image. Accordingly, it is recommended that the image providers or even the end-user select the optimal RPCs by such optimization-based method in order to achieve reasonable accuracy.

References

[1] Y. Zhang, Y. Lu, L. Wang, and X. Huang, "A new approach on optimization of the rational function model of high-resolution satellite imagery," *IEEE Trans. Geosci. Remote Sens.*, vol. 50, no. 7, pp. 2758–2764, 2012.

[2] V. O. Atak and M. O. Altan, "Geometric accuracy and feature compilation assessment of high resolution satellite images," in *Proc. ISPRS Commission IV Symp. Geospatial Databases Sustain. Develop.*, vol. 36. pp. 460–465, 2006.

[3] C. V. Tao and Y. Hu, "A comprehensive study of the rational function model for photogrammetric processing," *Photogramm. Eng. Remote Sens.*, vol. 67, no. 12, pp. 1347–1358, 2001.

[4] Y. Hu, V. Tao, and A. Croitoru, "Understanding the rational function model: Methods and applications," *Int. Arch. Photogramm. Remote Sens.*, vol. 20, no. 6, Jul. 2004.

[5] C. S. Fraser and H. B. Hanley, "Bias compensation in rational functions for IKONOS satellite imagery," *Photogramm. Eng. Remote Sens.*, vol. 69, no. 1, pp. 53–57, 2003.

[6] C. S. Fraser and H. B. Hanley, "Bias-compensated RPCs for Sensor Orientation of High-resolution Satellite Imagery," *Photogramm. Eng. Remote Sens.*, vol. 71, no. 8, pp. 909–915, 2005.

[7] L. Tengfei, J. Weili, and H. Guojin, "Nested regression based optimal selection (NRBOS) of Rational Polynomial Coefficients," *Photogramm. Eng. Remote Sens.*, vol. 80, no. 3, pp. 261–269, 2014.

[8] T. Long, W. Jiao, and G. He, "RPC Estimation via ℓ_1-norm-regularized least squares (L1LS)," *IEEE Trans. Geosci. Remote Sens.*, vol. 53, no. 8, pp. 4554–4567, Aug. 2015.

[9] A. Neumaier, "Solving III-conditioned and singular linear systems: A tutorial on regularization," *SIAM Rev.*, vol. 40, no. 3, pp. 636–666, 1998.

[10] T. Poggio, V. Torre, and C. Koch, "Computational vision and regularization theory," *Nature*, vol. 317, no. 6035, pp. 314–319, 1985.

[11] A. E. Hoerl and R. W. Kennard, "Ridge regression: Biased estimation for nonorthogonal problems," *Technometrics*, vol. 12, no. 1, pp. 55–67, 1970.

[12] C. V. Tao and Y. Hu, "Investigation of the rational function model," in *Proc. ASPRS Annu. Conv.*, May 2000, pp. 22–26.

[13] X. Yuan and X. Lin, "A method for solving rational polynomial coefficients based on ridge estimation," *Geomatics Inf. Sci. Wuhan Univ.*, vol. 33, no. 11, pp. 1130–1133, 2008.

[14] C. S. Fraser, G. Dial, and J. Grodecki, "Sensor orientation via RPCs," *ISPRS J. Photogram. Remote Sens.*, vol. 60, no. 3, pp. 182–194, 2006.

[15] M. Jannati and M. J. Valadan Zoej, "Introducing genetic modification concept to optimize rational function models (RFMs) for georeferencing of satellite imagery," *GISci. Remote Sens.*, vol. 52, no. 4, pp. 510–525, 2015.

[16] S. Yavari, M. J. Valadan Zoej, A. Mohammadzadeh, and M. Mokhtarzade, "Particle swarm optimization of RFM for georeferencing of satellite images," *IEEE Geosci. Remote Sens. Lett.*, vol. 10, no. 1, pp. 135–139, Jan. 2013.

[17] M. J. Valadan Zoej, M. Mokhtarzade, A. Mansourian, H. Ebadi, and S. Sadeghian, "Rational function optimization using genetic algorithms," *Int. J. Appl. Earth Observat. Geoinf.*, vol. 9, no. 4, pp. 403–413, 2007.

[18] X. Yuan and J. Cao, "An optimized method for selecting rational polynomial coefficients based on multicollinearity analysis," *Geomatics Inf. Sci. Wuhan Univ.*, vol. 6, no. 6, pp. 665–669, 2011.

[19] R. Tibshirani, "Regression shrinkage and selection via the lasso," *J. Roy. Statist. Soc. Ser. B (Methodol.)*, vol. 58, no. 1, pp. 267–288, 1996.

[20] S. S. Chen, D. L. Donoho, and M. A. Saunders, "Atomic decomposition by basis pursuit," *SIAM Rev.*, vol. 43, no. 1, pp. 129–159, 2001.

[21] B. Efron, T. Hastie, I. Johnstone, and R. Tibshirani, "Least angle regression," *Ann. Statist.*, vol. 32, no. 2, pp. 407–499, 2004.

[22] H. Zou and T. Hastie, "Regularization and variable selection via the elastic net," *J. Roy. Statist. Soc., B (Statistical Methodology)*, vol. 67, no. 2, pp. 301–320, 2005.

[23] E. Triantaphyllou, "Multi-criteria decision making methods," in *Multi-criteria Decision Making Methods: A Comparative Study*. Springer, 2000, pp. 5–21.

[24] E. Triantaphyllou, B. Kovalerchuk, L. Mann, and G. M. Knapp, "Determining the most important criteria in maintenance decision making," *J. Quality Maintenance Eng.*, vol. 3, no. 1, pp. 16–28, 1997.

[25] J. C. McGlone, "Manual of photogrammetry: American society for photogrammetry and remote sensing," Tech Rep., 2013.

[26] O. Rudenko and M. Schoenauer, "A steady performance stopping criterion for Pareto-based evolutionary algorithms," in *Proc. 6th Int. Multi-Objective Program. Goal Program. Conf.*, Apr. 2004, pp. 14–16.

[27] K. Deb, *Multi-Objective Optimization Using Evolutionary Algorithms*. Hoboken, NJ, USA: Wiley, 2001.

[28] C. M. Fonseca and P. J. Fleming, "Genetic algorithms for multiobjective optimization: Formulationdiscussion and generalization," in *Proc. ICGA*, vol. 93. Jul. 1993, pp. 416–423.

[29] C. M. Fonseca and P. J. Fleming, "An overview of evolutionary algorithms in multiobjective optimization," *Evol. Comput.*, vol. 3, no. 1, pp. 1–16, 1995.

[30] J. Horn, N. Nafpliotis, and D. E. Goldberg, "A niched Pareto genetic algorithm for multiobjective optimization," in *Proc. 1st IEEE Conf. Evol. Comput. IEEE World Congr. Comput. Intell.*, Jun. 1994, pp. 82–87.

[31] P. Capaldo, M. Crespi, F. Fratarcangeli, A. Nascetti, and F. Pieralice, "DSM generation from high resolution imagery: Applications with WorldView-1 and Geoeye-1," *Italian J. Remote Sens.*, vol. 44, no. 1, pp. 41–53, 2012.

[32] C. Fraser and M. Ravanbakhsh, "Georeferencing from Geoeye-1 imagery: Early indications of metric performance," in *Proc. ISPRS Hannover Workshop*, vol. 6. Jan. 2009.